International Journal of
Intelligent Systems and Applications in Engineering

ISSN:2147-6799 www.ijisae.org Original Research Paper

A Simple and Efficient Approach to Compute the Operating Frequency of Annular Ring Patch Antennas by Using ANN with Bayesian Regularization Learning Algorithm

Ahmet Kayabasi*[1], Ali Akdagli[2]

Accepted 3rd September 2016

Abstract:An annular ring patch antenna (ARPA) constructed by loading a circular slot in the center of the circular patch antenna is a popular microstrip antenna due to its favourable properties. In this paper, an application of artificial neural network (ANN) using bayesian regularization (BR) learning algorithm based on multilayer perceptron (MLP) model is presented for computing the operating frequency of annular ring ARPAs in UHF band. Firstly, the operating frequencies of 80 ARPAs having varied dimensions and electrical parameters were simulated with IE3DTM packaged software based on method of moment (MoM) in order to generate the data set for training and testing processes of the ANN model. Then ANN model was built with data set and while 70 simulated ARPAs and remaining 10 simulated ARPAs were employed for ANN model training and testing respectively. The proposed ANN model were confirmed by comparing with the suggestions reported elsewhere via measurement data published earlier in the literature. These results show that ANN model with BR learning algorithm can be successfully used to compute the operating frequency of ARPAs.

Keywords:*Annular ring patch antenna, operating frequency, Artificial neural network, Bayesian regularization learning algorithm.*

1. Introduction

The wireless communication systems are also moving towards the miniaturization very rapidly [1-2]. All these requirements of today's age wireless communication systems have led the antenna researchers to work on the various aspects of antenna designing with distinctive ideas of manufacturing and synthesis. Present portable communication and handheld devices inherently need miniaturized patch antennas (PAs). By using the substrate materials with high dielectric constant, the smaller antennas can be achieved but this gives rise to decrease the bandwidth and efficiency performances [1-2]. Thus, it is not an easy task to design a small PA managing the requirements of mobile communication devices. To cope such shortcomings of the traditional PAs, compact patch antennas (CPAs) which are formed by applying some modification such as shorting-pin/wall and slot-loading on the antenna structure, have been introduced in recent years [1]. Several slot loaded CPA configurations such as C [3], E [4-5], H [3, 6], L [7], rectangular ring [3] and annular ring [8] shapes have been presented in the literature as an alternative and effectively method to reduce the size of antenna.

Annular ring patch antennas (ARPAs) are miniaturized antenna constructed by loading a circular slot in the center of the circular patch. The size of the ARPA is substantially smaller than circular patch antenna (CPA) at the same operating frequency [8]. It can be appreciated that the average path length travelled by the current in the annular-ring patch is much longer than the corresponding circular patch for the lowest order mode [8]. Also, by choosing the inner and outer radius of the ring properly, both bandwidth broadening [8] and controlling the separation of resonant modes can be managed [9]. Due to these useful properties, it is the one of the most studied PAs. In the literature, the ARPA was theoretically investigated its resonator model in [10-13]. The mathematical tools such as vector Hankel transform, Galerkin's method and Green functions were greatly utilized in the analysis of the ARPAs [14-19]. Methods based on cavity model and transmission line model was presented to investigate some parameters such as the operating frequency, input impedance and bandwidth [20-26]. The experimental studies concerning the ARPA were also performed to confirm the theoretical calculations in [9-10, 15-16, 26-30]. It can be seen from the literature that these methods include rigorous calculation of Hankel and Fourier transforms and Bessel functions.

Analytical methods seems to be easier but they result in accurate solutions only for regular shapes of the patch, whereas the numerical electromagnetic computation methods are suitable for all shapes of the PA. However, the numerical methods require much more time in solving Maxwell's equations including integral and/or differential computations. So, it becomes time consuming since it repeats the same mathematical procedure even if a minor change in geometry is carried out. On the other hand, antenna designers prefer the easier approaches without requiring much rigorous computations and consuming time.

Over a last decade artificial neural network (ANN) adopts remarkable importance in field of wireless communication due to its fast and accurate modelling, simulation, and optimization. In ANN model, we can use measured, simulated, and calculated data for training. Trained ANN model predicts accurate operating

[1]*Engineering Faculty, Department of Electrical-Electronics Engineering, Karamanoglu Mehmetbey University 70100, Karaman, Turkey*
[2]*Engineering Faculty, Department of Electrical-Electronics Engineering, Mersin UniversityCiftlikkoy, Yenisehir, 33343, Mersin, Turkey*
** Corresponding Author:Email: ahmetkayabasi@kmu.edu.tr*
Note: This paper has been presented at the 3rd International Conference on Advanced Technology & Sciences (ICAT'16) held in Konya (Turkey), September 01-03, 2016.

frequency for every small variation in the geometry both for thin and thick substrates. The purpose behind the training of ANN model is to minimize the error between actual output and reference output. The use of ANN in computing resonant frequency of CPAs have been proposed in [5-6].

In this study, a method of feed forward back propagation ANN (FFBP-ANN) with bayesian regularization (BR) learning algorithm [31] based on multilayered perceptron (MLP) model has been applied to compute the resonant frequencies of ARPAs. The operating frequency values of 80 ARPAs corresponding most of UHF band covering GSM, LTE, WLAN and WiMAX applications were determined by the electromagnetic simulator IE3DTM using method of moment (MoM) [32]. The simulation parameters of 70 ARPAs representing the overall problem space were used to training and the remaining 10 were then employed to test the accuracy. The results of the ANN model obtained in this study was confirmed by comparing with the measurement results published earlier in the literature [9, 10, 15, 16, 26–30].

2. Annular Ring Patch Antenna and Simulation Phase

As shown in (Figure.1), ARPA has an annular patch formed by loading a circular slot with radius a_i on a circular patch of radius a_o on the substrate having relative dielectric constant ε_r overall on the ground plane.

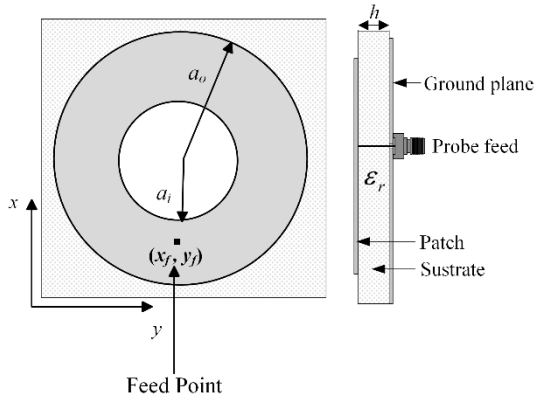

Figure1. Geometry of ARPA

In order to determine the operating frequency values, the simulations were performed by means of the IE3D™ packaged software for 80 ARPAs having various parameters of antenna dimensions and dielectric constants listed in Table 1. The antennas operate among 0.66 – 3.71 GHz corresponding to the UHF band.

In the simulations, the antennas were supposed to a probe feed with 50 Ω. For meshing process, cell/wavelength rate values were assumed as 40 in limit of 4 GHz. The built in optimization module of the IE3DTM was utilized to determine the feed point which gives the best return loss value with the objective function S11(dB) < −10 for the operating frequencies at TM11 mode.

3. Modelling of the ANN for the Computation the Operating Frequency of ARPAs

ANN is one of the popular intelligence technique in solving engineering and mathematical problems. An ANN consists of neurons which are organized into different layers. These neurons contain non-linear type of functional, they are mutually connected by very much similar synaptic weights. During the learning process, these synaptic weights could be weakened or strengthened and therefore helping the data to be kept in the ANN. Different learning algorithms (LAs) are used for ANN networks. Some famous type of different backpropagation LAs are Levenberg Marquardt (LM), Bayesian regularization (BR), cyclical order incremental update (COIU), Powel-Beale conjugate gradient (PBCG), Fletcher-Powel conjugate gradient (FPCG), Polak-Ribiere conjugate gradient (PRCG), one step secant (OSS) and scaled conjugate gradient (SCG) [31].

Table 1. Dimensions and dielectric constants of the simulated ARPAs

Number of simulations	Patch dimensions (mm)			
	a_o *Outer radius*	a_i *Inner radius*	h	ε_r
4x20	15	2, 4, 6, 8, 10	3.175	2.2
	20	3, 6, 9, 12, 15	3.175	2.2
	25	4, 8, 12, 16, 20	3.175	2.2
	30	5, 10, 15, 20, 25	3.175	2.2
	15	2, 4, 6, 8, 10	2.5	9.8
	20	3, 6, 9, 12, 15	2.5	9.8
	25	4, 8, 12, 16, 20	2.5	9.8
	30	5, 10, 15, 20, 25	2.5	9.8
	15	2, 4, 6, 8, 10	1.57	2.33
	20	3, 6, 9, 12, 15	1.57	2.33
	25	4, 8, 12, 16, 20	1.57	2.33
	30	5, 10, 15, 20, 25	1.57	2.33
	15	2, 4, 6, 8, 10	0.64	4.5
	20	3, 6, 9, 12, 15	0.64	4.5
	25	4, 8, 12, 16, 20	0.64	4.5
	30	5, 10, 15, 20, 25	0.64	4.5

In this study, the BR algorithm was used in ANN model as learning algorithm. BR learning algorithm updates the weight and bias values according to the LM optimization and minimizes a linear combination of squared errors and weights [33]. It also modifies the linear combination so that at the end of training the resulting network has good generalization qualities.

3.1. Training Stage of the ANN Model

The physical dimensions (a_o, a_i, and h) and dielectric constant values (ε_r) of the simulated ARPAs were given as inputs and their respective operating frequency values of IE3D™ were given as output to the ANN model. While 70 of 80 ARPAs were employed for training phase, others 10 were used for test the models. After several trials, a hidden layer with four neurons, which yields satisfactorily results was employed. Thus, MLP ANN model having one input layer with four neurons, one hidden layer with four neurons and one output layer with one neuron was constructed, as shown in (Figure.2), where f_{IE3D} and f_{ANN} are the operating frequencies computed by IE3D™ and ANN model, respectively.

In the ANN model trained with BR learning algorithm, "tangent sigmoid" function was used for both input and hidden layers, whereas "purelin" function was utilized for output layer. The parameters of the ANN model used in this work are listed in Table 2. The topology of the training process and calculation of average percentage error (APE) are illustrated for ANN model in (Figure.3). According to (Figure.3), the value of APE for the operating frequencies computed by the ANN model was obtained as 0.437% for the 70 ARPAs' training data. The training results of the ANN model together with the results of IE3D™ were

given in (Figure.4).

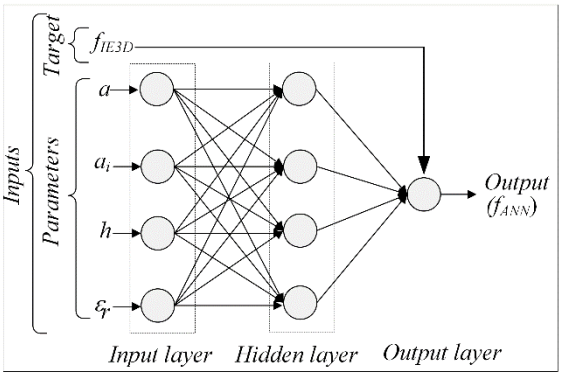

Figure 2. Geometry of ARPA The block diagram of ANN model

Table 2. The ANN parameters

Parameters	Value
Number of input	4
Number of output	1
Epochs	500
Seed value	662862703
Minimum gradient descent	10^{-10}
Momentum parameter (μ)	0.0001
μ increment	4
μ decrement	0.1
Maximum μ	10^{10}

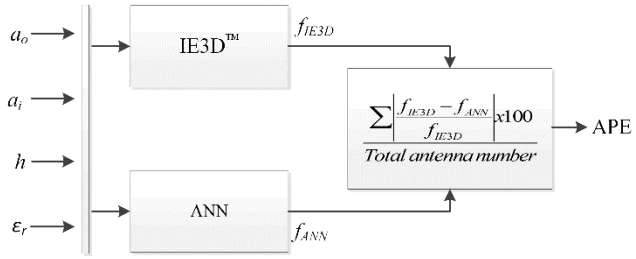

Figure 3. The calculating of APE for ANN model

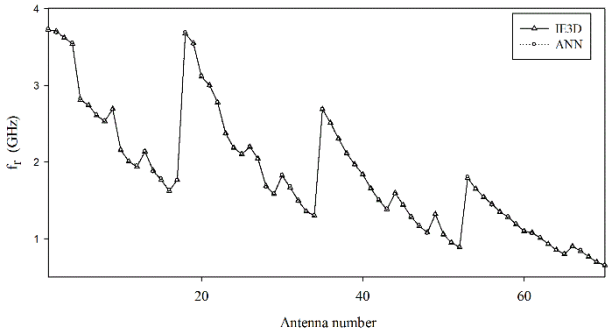

Figure 4. The comparative results of the simulation and ANN model for training phase

3.2. Testing Stage of the ANN Model

To test the performances of the ANN model constructed here, 10 simulated ARPAs whose electrical and psychical parameters listed in Table 3 are employed. The predicted operating frequency results and APE value of the ANN model with BR learning algorithm are tabulated in Table 4. For further comparison, the numerical results of several methods previously published in the literature [12-13, 25-26] are also listed in Table 4. It is apparent from Table 4 that, the ANN model give the remarkable results in comparison with those calculated by the methods presented in the literature [12-13, 25-26].

Table 3. The physical and electrical parameters of 10 simulated ARPAs for test process

Antenna number	Antenna parameters				
	Patch dimensions (mm)				
	a_o	a_i	h	ε_r	h/λ_d
1	15	4	2.5	9.8	0.045
2	15	6	1.57	2.33	0.027
3	15	10	3.175	2.2	0.056
4	20	3	0.64	4.5	0.009
5	20	6	1.57	2.33	0.021
6	20	15	2.5	9.8	0.027
7	25	4	3.175	2.2	0.035
8	25	12	1.57	2.33	0.015
9	30	10	0.64	4.5	0.005
10	30	20	3.175	2.2	0.024

Table 4. The operating frequencies and ape values for test process

Operating Frequencies (GHz)					
f_{IE3D}	f_{ANN}	Calculated by			
	BR	[12]	[13]	[25]	[26]
1.734	1.744	1.735	1.814	1.813	2.888
3.323	3.329	3.265	3.181	3.181	3.749
3.563	3.498	2.917	2.843	2.844	2.396
2.006	1.965	1.995	2.025	2.025	5.234
2.594	2.600	2.576	2.534	2.535	3.700
1.033	1.035	1.041	1.027	1.026	0.804
2.258	2.300	2.135	2.354	2.355	5.748
1.833	1.819	1.832	1.785	1.785	1.854
1.189	1.190	1.193	1.160	1.159	1.564
1.547	1.601	1.420	1.395	1.395	1.175
APE (%)	1.118	3.595	5.207	5.217	54.910

In order to verify the accuracy and validity for the crosscheck, the operating frequency results obtained by means of the ANN model learning with BR has been compared with those of the methods reported elsewhere [12-13, 25-26] over several measurement data of ARPAs published earlier in literature [9-10, 15-16, 26-30]. Table 5 gives the operating frequency values predicted with the ANN model with BR and calculated with the methods given in [12-13, 25-26], and also the their respective APE values according to the measurement parameters [9-10, 15-16, 26-30]. It should be noted that these measurement parameters were not employed for training the ANN model. As can be seen from the Table 5, the methods proposed for operating frequency of the ARPA yield the comparable results, however, some calculations are in good agreement with some measured data, and others are far off. But, the operating frequency results of the ANN providing the least APE value within 1% are closer to the measurement ones for the most cases. The results achieved here show that the ANN can effectively be employed to estimate the operating frequency of ARPAs.

Table 5. The measured and calculated operating frequencies for ARPAs

	Antenna parameters							Operating Frequencies (GHz)			
	Dimensions (mm)							Calculated by			
	a_o	a_i	h	ε_r	h/λ_d	$f_{measured}$	f_{ANN}	[12]	[13]	[25]	[26]
[9]	50	25	1.59	2.32	0.007	0.878	0.873	0.886	0.85	0.854	0.877
[10]	20	10	3.18	2.32	0.040	2.450	2.524	2.337	2.171	2.149	2.297
[15]	50	25	1.59	2.32	0.007	0.891	0.873	0.886	0.850	0.854	0.877
[16]	14.2	7.1	0.355	2.65	0.006	2.880	2.880	2.907	2.790	2.811	2.882
[26]	17.2	8.6	1.6	4.20	0.022	1.989	2.048	2.035	1.850	1.855	1.997
[27]	70	35	1.59	2.32	0.005	0.625	0.624	0.627	0.600	0.609	0.622
[28]	70	35	1.59	2.3	0.005	0.626	0.625	0.629	0.610	0.612	0.625
[29]	30	10	0.8	4.4	0.007	1.243	1.211	1.213	1.150	1.171	1.590
[30]	35	17.5	1.53	4.3	0.010	0.940	0.949	0.954	0.890	0.897	0.941
[30]	17.5	8.75	1.53	4.3	0.021	1.960	1.975	1.972	1.790	1.801	1.936
APE (%)							1.328	1.464	5.830	5.158	3.820

As an important matter of the fact that, although the method of ANN seems more complicated as compared to the other ones, it provides the more accurate and relatively simple way since it requires neither sophisticated functions of mathematical transformations nor rigorous expertness to determine the unknown parameters in any problem including highly nonlinearity. The training process is once completed in a few minutes by properly choosing the network parameters and the learning method, one can easily compute any parameters of interest in microseconds.

4. Conclusion

In this paper, an application of ANN model which have been used BR learning algorithm is successfully implemented for the prediction of accurate operating frequency of ARPAs. IE3D™ simulation software based on MoM was used to define operating frequency of 80 ARPAs. ANN model, physically and electrical parameters of 70 ARPAs were utilized training data, 10 ARPAs were utilized for the test. It was seen that computed results with ANN for training and test data are in a good agreement with the simulation results. This method achieved the more accurate results as compared to those of the methods proposed in the literature. This ANN approach is simple and fast modelling which produces more accurate results for the operating frequency of the ARPAs with less computational time and least errors. The most important advantages ANN model is accuracy and easy to implement for the engineering problems which include the high nonlinearity.

References

[1] K. Wong (2002). Compact and broadband microstrip antennas. John Wiley & Sons, Inc.

[2] G. Kumar and K. P. Ray (2003). Broadband microstrip antennas, Norwood: Artech House.

[3] A. A. Deshmukh and G. Kumar (2007). Formulation of resonant frequency for compact rectangular microstrip antennas. Microwave and Optical Technology Letters. 49 (2) 498–501.

[4] A. A. Deshmukh, N. V. Phatak, S. Nagarbovdi and R. Ahuja(2013). Analysis of Broadband E-shaped Microstrip Antennas. International Journal of Computer Applications. 80 (7) 24– 29.

[5] A. Akdagli, A. Toktas, A. Kayabasi and I. Develi (2013). An application of artificial neural network to compute the resonant frequency of E-shaped compact microstrip antennas. Journal of Electrical Engineering-Elektrotechnicky Casopis. 64 (5) 317–322.

[6] A. Kayabasi, M. B. Bicer, A. Akdagli and A. Toktas (2011) Computing resonant frequency of H-shaped compact microstrip antennas operating at UHF band by using artificial neural networks. Journal of the Faculty of Engineering and Architecture of Gazi University.26 833–840.

[7] Z. N. Chen (2000). Radiation pattern of a probe fed L-shaped plate antenna. Microwave and Optical Technology Letters. 27 410–13.

[8] W. Chew (1982). A broad-band annular-ring microstrip antenna. IEEE Transactions on Antennas and Propagation. 30 (5) 918–922.

[9] J. S. Dahele, K. F. Lee and D. Wong (1987). Dual-frequency stacked annular-ring microstrip antenna. IEEE Transactions on Antennas and Propagation. 351281–1285.

[10] I. J. Bahl, S. S. Stuchly and M. A. Stuchly (1980). A new microstrip radiator for medical applications. IEEE Transactions on Microwave Theory and Techniques. 28 1464–1469.

[11] I. Wolff and N. Knoppik (1971). Microstrip ring resonator and dispersion measurement on microstrip lines. Electronics Letters. 7 779–781.

[12] S. G. Pintzos and R. Pregla (1978). A simple method for computing the resonant frequencies of microstrip ring resonators. IEEE Transactions on Microwave Theory and Techniques. 26809–813.

[13] Y. S. Wu and F. J. Rosenbaum (1973). Mode chart for microstrip ring resonators. IEEE Transactions on Microwave Theory and Techniques. 21487–489.

[14] S. M. Ali, C. Weng and J. Kong (1982). Vector Hankel transform analysis of annular-ring microstrip antenna. IEEE Transactions on Antennas and Propagation. 30 637–644.

[15] Z. Fan and K. F. Lee (1991). Hankel transform domain analysis of dual-frequency stacked circular-disk and annular-ring microstrip antennas. IEEE Transactions on Antennas and Propagations. 29867–870.

[16] H. Liu and X. F. Hu (1996). An improved method to analyse the input impedance of microstrip annular-ring antennas. Journal Electromagnetic Waves and Applications. 10827–833.

[17] H. Liu and X. F. Hu (1996). Input impedance analysis of microstrip annular ring antenna with thick substrate. Progress In Electromagnetic Research. 12177–204.

[18] C. S. Gurel and E. Yazgan (2010). Resonant frequency

analysis of annular ring microstrip patch on uniaxial medium via Hankel transform domain immittance approach. Progress In Electromagnetic Research. 11,37–52.

[19] A. Motevasselian (2011). Specteral domain analysis of resonant characteristics and radiation patterns of a circular disk and annular ring microstrip antenna on uniaxial substrate. Progress In Electromagnetic Research. 21 237–251.

[20] W. F. Richards, O. Jai-Dong and S. Long (1984). A theoretical and experimental investigation of annular, annular sector, and circular sector microstrip antennas. IEEE Transactions on Antennas and Propagations. 32 864–867.

[21] A. K. Bhattacharyya and R. Garg (1985). Input impedance of annular ring microstrip antenna using circuit theory approach. IEEE Transactions on Antennas and Propagations. 33369–374.

[22] S. E. El-Khamy, R. M. El-Awadi and E. B. A. El-Sharrawy (1986). Simple analysis and design of annular ring microstrip antennas. Microwaves, Antennas and Propagation, IEE Proceedings H.133 198–202.

[23] J. Gomez-Tagleand and C. G. Christodoulou (1997). Extended cavity model analysis of stacked microstrip ring antennas. IEEE Transactions on Antennas and Propagations. 45 1626–1635.

[24] V. Sathi, C. H. Ghobadi and J. Nourinia (2008). Optimization of circular ring microstrip antenna using genetic algorithm. International Journal of Infrared and Millimeter Waves. 29 897–905.

[25] I. J. Bahl and S. S. Stuchly (1992). Closed-form expressions for computer-aided design of microstrip ring antennas. International Journal of Infrared and Millimeter Wave Computer-Aided Engineering. 2144–154.

[26] R. Kumar and D. C. Dhubkarya (2011). Design and analysis of circular ring microstrip antenna. Global Journal of Researches In Engineering. 11 (1).

[27] J. S. Dahele and K. F. Lee (1982). Characteristics of annular-ring microstrip antenna. Electronics Letters. 181051–1052.

[28] K. F. Lee, J. S. Dahele and K. Y. Ho (1983). Annular-ring and circular-disc microstrip antennas with and without air gaps. 13th European Microwave Conference. 389–394.

[29] J. S. Row (2004). Dual-frequency circularly polarized annular-ring microstrip antenna. Electronics Letters. 40153–154.

[30] J. Shinde, P. Shinde, R. Kumar, M. D. Uplane and B. K. Mishra (2010). Resonant frequencies of a circularly polarized nearly circular annular ring microstrip antenna with superstrate loading and airgaps. In: Kaleidoscope: Innovations for Future Networks and Services. 1–7.

[31] M. Zandieh, A. Azadeh, B. Hadadi and M. Saberi (2009). Application of neural networks for airline number of passenger estimation in time series state. Journal of Applied Science. 9 (6) 1001–1013.

[32] R. F. Harrington (1993). Field computation by moment methods, Piscataway. NJ, IEEE Press.

[33] D. J. C. Mackay (1992). Bayesian interpolation. Neural Computation. 4415–447.